Uncertainty Estimation on Active Surface-Waves Based Tests

Esteban Sáez[1,5#], *Felipe* Hernández[2], *Rocío* Vega[1], *Juan Carlos* Tiznado[1], *Ricardo* Gallardo[2], *Felipe* Leyton[3], *Gonzalo* Montalva[4] and *César* Pastén[3]

[1]*Pontificia Universidad Católica de Chile, Department of Structural and Geotechnical Engineering, Av. Vicuña Mackenna 4860, Macul, Santiago, Chile*
[2]*Pontificia Universidad Católica de Valparaíso, Department of Civil Engineering, Av. Brasil 2950, Valparaíso*
[3]*Universidad de Chile, Department of Civil Engineering, Beauchef 850, Santiago*
[4]*Universidad de Concepción, Department of Civil Engineering, Edmundo Larenas 219, Concepción*
[5]*CIGIDEN -National Research Center of Integrated Natural Disaster Management, Av. Vicuña Mackenna 4860, Macul, Santiago, Chile*
[#]*Corresponding author: esaezr@uc.cl*

ABSTRACT

Geophysical methods based on surface waves have become very popular in recent decades due to their versatility and reduced cost of execution compared to other invasive techniques. Due to space constraints in urban environments, measurements with linear arrays using active and passive techniques are usually combined to reach the exploration depth required by seismic site classification regulations. Although several good practice guidelines have been developed for performing this type of geophysical explorations, one of the remaining major challenges is to relate the results of these explorations to uncertainty metrics. In the case of active tests, there are effects associated with the filtering method used to eliminate the near and far-field effects, as well as other difficulties related to higher Rayleigh-modes or heterogeneities of the site.
In this paper, we study the effect of body waves unavoidably induced in active tests on the proper determination of the dispersion curve of a site. For this purpose, active tests are carried out using triaxial geophones to extract from the records the motion effectively corresponding to Rayleigh waves by means of the Normalized Inner Product (NIP) technique. The results show that the effects of body waves are negligible for frequencies above about 8 Hz, but below this value, in the transition zone with ESPAC passive tests, the differences can be more significant. These results are used to introduce uncertainty indicators in this type of explorations.

Keywords: surface wave methods; active tests; Rayleigh waves; uncertainty in geophysical methods.

1. Introduction

Geophysical methods based on surface waves have become very popular in recent decades due to their versatility and reduced cost of execution compared to other invasive techniques. Indeed, many seismic design codes suggest the use of these methods to estimate main parameters for seismic site classification (e.g., Vs30). In the case of Chile, geophysical methods based on surface waves began to be routinely applied after the Mw 8.8, 2010 Maule earthquake.
Due to space constraints in urban environments, measurements with linear arrays using active and passive techniques are usually combined to reach the exploration depth required by seismic site classification regulations. Although several good practice guidelines have been developed for performing this type of geophysical explorations (Humire et al, 2015; Foti et al. 2018) one of the remaining major challenges is to relate the results of these explorations to uncertainty metrics. For example, in the case of passive surveys, some indicators can be obtained as part of data processing; particularly from dispersion curve variability associated with the uncertainty in the direction of incidence of surface waves. In the case of active tests, there are effects associated with the filtering method used to eliminate the near and far-field effects (e.g. Yoon and Rix, 2009), as well as other difficulties related to higher Rayleigh-modes (e.g. Tremblay and Karray, 2019) or heterogeneities of the site. Other effects such as the characteristics of the source, the type of sensors and their geometrical distribution, as well as the level of background ambient noise, also play a role in the reliability of the tests and the quality of their results.
In the case of rigid to medium stiff sites, active testing requires relatively long spreads and powerful active sources to have a satisfactory signal-to-noise ratio across the entire array. Since usual active sources such as seismic hammers do not meet this requirement, in practice, active tests are often combined with ambient noise measurements through the same array. Among the available methods for analysing these passive linear records, in the author's experience (e.g. Maringue et al, 2022), the Extended SPAC (ESPAC) proposed by Hayashi (2008) provides the best results. Since these methods are usually combined to obtain a Vs30 value for the explored site, in general, the objective of the survey

is to describe the Rayleigh dispersion curve between a wavelength of 5 and 90 m, approximately. On rigid sites, this is usually achieved with 4.5 Hz vertical geophones and line arrays of about 70-80 or more meters long. In practice, these surveys are usually performed with 12 to 24-channel equipment, depending on the manufacturer. Although this procedure usually gives satisfactory results, it does not allow to directly obtain uncertainty metrics related to the dispersion curve. Therefore, there is need for developing control procedures, ideally in the field, for both the reliability of results and unanticipated complexities of the site that might require a modification of the survey plan.

Among the different sources of uncertainty, this paper focused on the effect of body waves unavoidably induced in active tests. For this purpose, active tests were carried out using 0.5 Hz and 1 Hz triaxial geophones in several sites located in the cities of Coquimbo and La Serena in northern Chile. In these cities, the sites are composed mainly of medium dense sands to gravels (i.e., relatively stiff soils). To extract from the records the motion effectively corresponding to Rayleigh waves, we used the Normalized Inner Product (NIP) technique (Meza-Fajardo, Papageorgiou and Semblat, 2015). To have an active source of higher energy that could generate a perceptible motion along the entire length of the spread, a mechanical source consisting of a 100 kg weight dropped from a height of 2.5 m was developed. In parallel to each test, a standard reference measurement was made with 24 vertical 4.5 Hz geophones where the NIP technique cannot be applied. The following sections describe in more detail the field procedure, the analysis of records, and the main findings of this study.

2. Methodology

2.1. Field work

The purpose was to perform active tests at sites of varying stiffness. At each of these sites, two acquisition systems were deployed in parallel:

- A wired seismometer of 24 vertical 4.5 Hz geophones at regular separation (Figure 1a). A uniform separation of 5m was used between sensors, i.e., spreads of 115 m. In this case, Geometrics Geode® equipment was used, including a trigger.
- A total of eight independent SARA Electronics Instruments® triaxial sensors. Two Terrabot 1 Hz sensors (T1 and T2 in Figure 1b) and six SSBH05 0.5 Hz sensors connected to SL06 digitisers were used (F1 to F9 sensors in Figure 1b). The first two sensors were spaced at the same spacing as the first two sensors of 4.5 Hz, and then increased in additional one additional spacing as the distance to the source increased. For example, for a regular spacing of 5 m, the second and third triaxial seismometers were spaced 10 m apart and so on.

A 100 kg mass dropped from a height of 2.5 m was used as source (Figure 1c). In the case of the Geode®, a trigger was used to record 2 seconds of motion. In the case of the triaxial seismometers, a continuous synchronised recording was made between sensors. All tests were sampled at 200 Hz. The source was located outside the array at one and two times the 4.5 Hz sensor spacing. In general, between 5 to 8 tests were performed per source location. Once the active tests had been carried out, an ambient noise recording was made for approximately 1 hour.

(a) (b) (c)

Figure 1. Example of field work (Id-18 according to Table 1): (a) vertical sensors together with triaxial seismometers; (b) deployment of sensors in the field, the stars indicate the location of the source; (c) 100 kg seismic source.

The sites chosen for this paper are listed in Table 1. This table indicates the corresponding Vs30 value and the predominant soils as a way of characterising the average stiffness of the site. Vs30 values were estimated combining all available information, i.e., active, linear passive, and two-dimensional passive tests (not presented in this paper). The Id numbers are not correlative as they are part of a larger project where around 30 sites in different cities of the country were characterised.

Table 1. Characterised sites.

Id	Spacing (m)	Predominant soils	Vs30 (m/s)
15 – Lighthouse	5	Medium dense saturated sands	276.5
16 –Pedro de Valdivia Park	5	Gravels	451.7
18 – CENDYR	5	Residual soils	507.7
21 – Coquimbo Billboard	5	Sands and gravels	359.3

2.2. Data processing

For active tests, the f-k (frequency-wavenumber analysis) method (Lacoss et al. 1969; Kværna and Ringdahl 1986; Wathelet 2005) as implemented in the GEOPSY package (Wathelet 2002-2011) was used for data processing. In the case of linear ambient measurements, the ESPAC analysis (Hayashi 2008) as implemented in Seisimager® code was used. In the case of triaxial recordings, Seismowin® software was used to synchronise the sensors, isolate each experiment, and make the deconvolutions with the response curves of each instrument to recover particle velocities.

In practice, wired equipment with 12 or more vertical sensors is used for active testing. Under these conditions, it is assumed that the recorded motion consists of mainly Rayleigh wave and typically the sensors closest to the source are removed to avoid the contribution of body waves (e.g. Yoon and Rix, 2009). There are several ways to avoid these near field effects and a comprehensive overview of different alternatives is presented in Tremblay and Karray (2019). In this research, a different approach is followed to quantify the differences between considering the total recorded motion versus a filtered alternative to extract the proportion attributable to Rayleigh wave. There are several approaches in the literature to extract specific wavefields from recorded seismic motions, in particular, surface wave. Many of these methods have been developed to study, for example, sedimentary basin effects from seismic event records. According to Soto (2023), there are two main groups of such techniques: (i) those that perform a polarization analysis from single stations records; (ii) and the ones that use multiple stations to compute a coherent summation of signals of the same polarization (Greenhalgh et al., 2008). For this phase of the research, we focused mainly on single-station techniques. Among the available approaches, the Normalized Inner Product or NIP (Meza-Fajardo et al., 2015) and the Six Degrees-of-Freedom Polarization Analysis or 6CPol (Sollberger et al., 2018) stand out. However, given the characteristics of the sensors used, only NIP is feasible to apply to our field data. NIP is a time-frequency polarization analysis based on the correlation between two orthogonal components to separate surface waves from the total recorded motion. The method allows to identify prograde and retrograde Rayleigh wave by minimizing the correlation coefficient between vertical and horizontal components in a time-frequency domain using the Stockwell transform (Stockwell et al., 1996). Since the source location is known for this study, the triaxial instruments were oriented so that one of the horizontal components followed the propagation direction through the linear array (i.e., the analysis was then performed in that vertical plane). The out-of-plane component can also be used to extract the Love wave, which will be analysed in future stages of the study. Once the prograde and retrograde component of the Rayleigh wave extracted, the estimation of the site dispersion curve was repeated using the f-k method.

3. Results

3.1. Rayleigh wave extraction

As an example, the Figure 2 shows the vertical component of the particle velocity (in mm/s) at three different triaxial geophones for the site Id 15. Very close to the source (F3Z), the vertical amplitude of the recorded motion is significantly larger than the Rayleigh polarizations, which accounts for the contribution of the body waves. At this distance, the waveform appears to be composed of a single wave group. The prograde Rayleigh component appears to have a shorter duration than the retrograde polarization and the total vertical motion. Note that these experiments were not triggered and, therefore, the time prior to the arrival of the significant amplitude of motion was manually adjusted for processing.

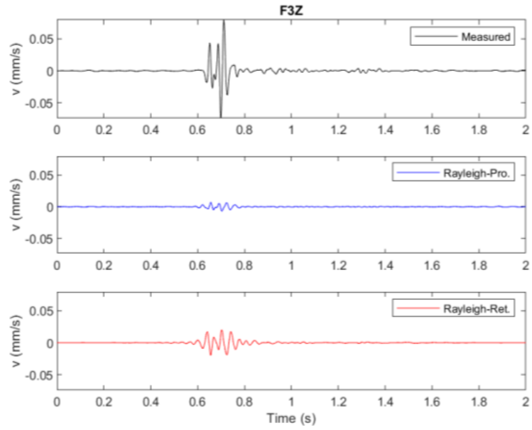

(a)

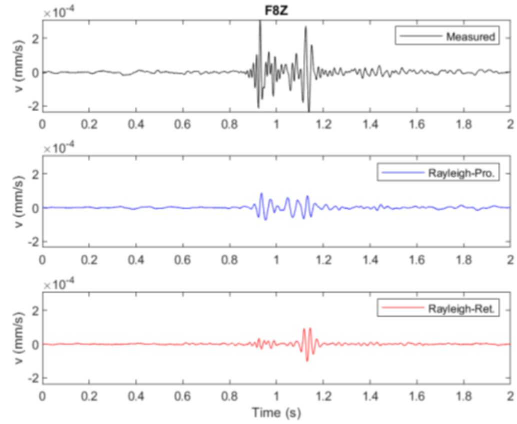

(b)

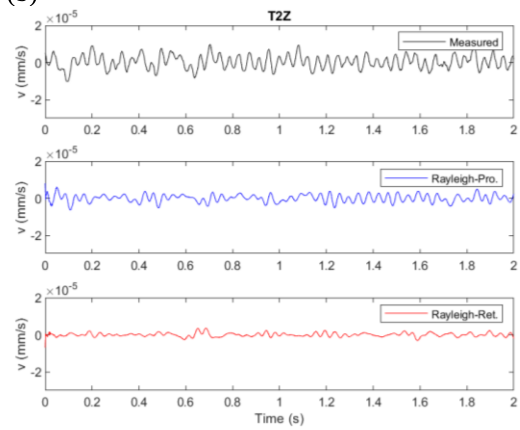

(c)

Figure 2. Example of recorded and filtered waveforms after applying the NIP procedure: (a) F3Z-vertical component recorded at 5m of the source; (b) F8Z-vertical component recorded at 50 m of the source; (c) T2Z-vertical component recorded at 125m of the source.

At about half of the linear array (F8Z), the total motion has attenuated significantly, while the Rayleigh waves now exhibit peak amplitudes of about 30% of the total vertical motion. On the other hand, the waves have now separated into two groups during propagation, suggesting that the mass used for impact may have rebounded after hitting the ground. Finally, at the end of the array and at more than 120 m from the source (T2Z), the record is essentially composed of ambient noise and the impact is no longer distinguishable.

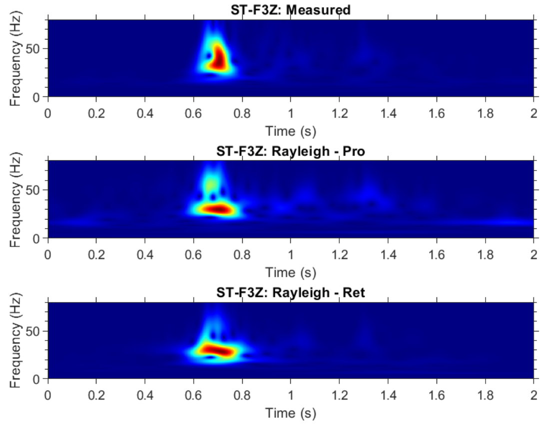

(a)

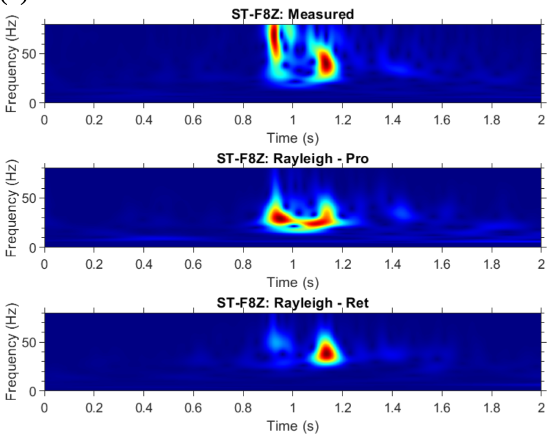

(b)

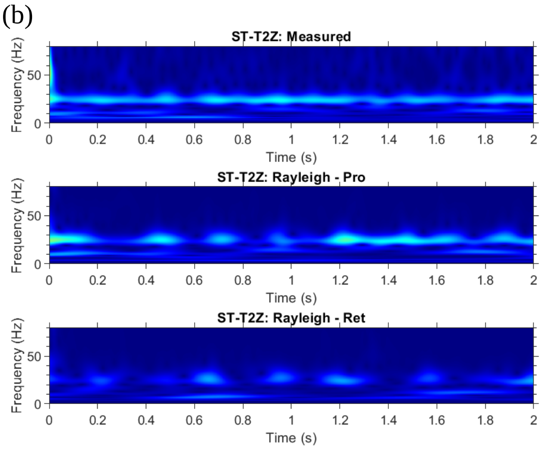

(c)

Figure 3. Stockwell transform of recorded and filtered waveforms after applying NIP procedure: (a) F3Z-vertical component recorded at 5m of the source; (b) F8Z-vertical component recorded at 50 m of the source; (c) T2Z-vertical component recorded at 125m of the source.

To illustrate the differences in frequency content, Figure 3 shows the Stockwell transforms of the same waveforms. Near the source (F3Z), the Rayleigh wave frequency range is smaller than the total motion. While the total motion covers a range between 30 and 60 Hz approximately, the prograde Rayleigh wave tends to concentrate around two frequencies (30 Hz and 60 Hz). In the case of the retrograde Rayleigh wave, the frequency content is similar to the prograde polarization.

At the centre of the array (F8Z), the total motion is composed of two wavefronts. The first propagates at a higher frequency (65Hz), while the second is slower and located approximately at 30 Hz. When compared against the Stockwell transforms of the Rayleigh polarisations, the first seems to be much more influenced by the prograde polarization, while the second has both prograde and retrograde Rayleigh wave components. In this case, the retrograde polarisation has a slightly higher frequency content than the prograde and dominates the second wavefront.

Finally, far away from the source, no contribution from source-induced motion is distinguishable and the ambient noise in this time window is mainly characterised by Rayleigh waves below 30 Hz with a nearly constant amplitude. Two frequencies stand out during this time window: one below 10 Hz and one close to 25 Hz.

3.2. Amplitude decay

To illustrate the average contribution of each Rayleigh polarization to the measured motion, the analysis was repeated for each experiment at each site listed in Table 1. Different source positions allowed to explore different source-receiver distances for the same sensor. The graphs in the Figure 4 show the mean value as well as the standard deviation obtained from the combination of all experiments at the same site.

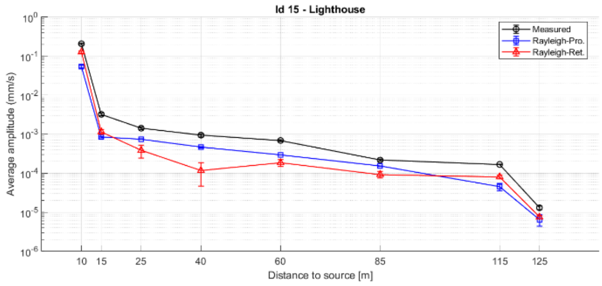

(a)

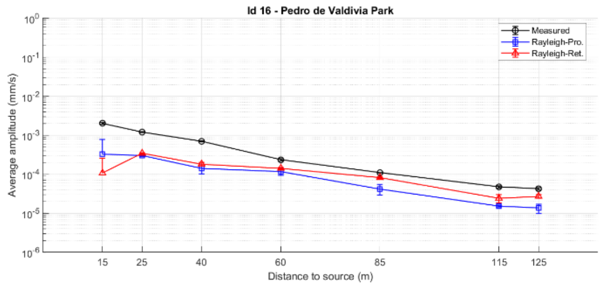

(b)

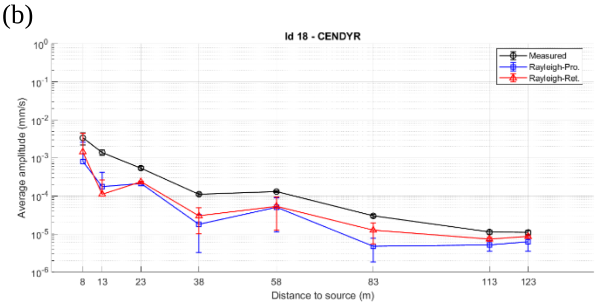

(c)

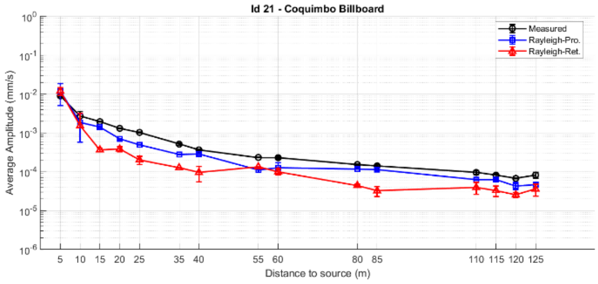

(d)

Figure 4. Decay of the maximum amplitude of the vertical particle velocity at different distances from the source: (a) Site Id 15 – Lighthouse; (b) Site Id 16 – Pedro de Valdivia Park; (c) Site Id 18 – CENDYR; (d) Site 21 – Coquimbo Billboard.

It can be noted that the maximum amplitudes near the source (<15m) are significantly higher for the softest site (Id 15) compared to the stiffer sites. However, for distances greater than approximately 15m, the amplitudes become much more similar, regardless of the stiffness of the site. Note that a controlled mechanical source was used to have approximately the same energy at all sites and in all tests. While there is some variability, the motion attenuation follows a roughly constant rate for distances greater than 15m up to about 115m. For greater distances to source, the procedure yields rather erratic results, suggesting that the signal-to-noise ratio is too small to be accurately distinguished.

If we focus on distances to source between 15 and 115m, it is observed that the variability of the measured vertical velocity amplitude is very low, being practically a constant value. In contrast, the application of NIP generates Rayleigh wave amplitudes that are more variable, particularly at sites Id 15 and Id 18. Note that site Id 18 was particularly far from the city and there was a very low level of ambient noise.

In terms of decay rate with distance from the source, both Rayleigh waves and the measured motion follow a similar trend, except for site Id 18 which is more erratic. Complementary information (MASW2D tests and seismic refractions) shows that in this site the most significant impedance contrast depth is steeply sloping as the site is located on a cut in a hillside. Further analysis is underway to define whether this effect could explain the higher variability of the maximum amplitudes of the surface waves induced by the seismic source.

3.3. Dispersion curve estimation

Finally, f-k analysis was performed on the three sets of available waveforms: the measured motion and the Rayleigh polarisations obtained with the application of the NIP technique. In each case, the same criteria were adopted to eliminate the first and eventually the second sensor closest to the source to avoid near-field effects or tests that had saturated these sensors.

For comparison purposes, the dispersion curve was also obtained using the 24 vertical geophones of the Geode® equipment, both during the execution of the active tests (labelled as MASW) and as a result of the analysis of one-hour ambient vibration recording (indicated as ESPAC). Both, MASW and ESPAC curves, were obtained from the measured motion as indicated in the plots of the first column of Figure 5. Therefore, it is to be expected that these curves do not perfectly follow the spectrum maxima when isolating the prograde and retrograde Rayleigh component, i.e. plots of the second and third columns of this figure.

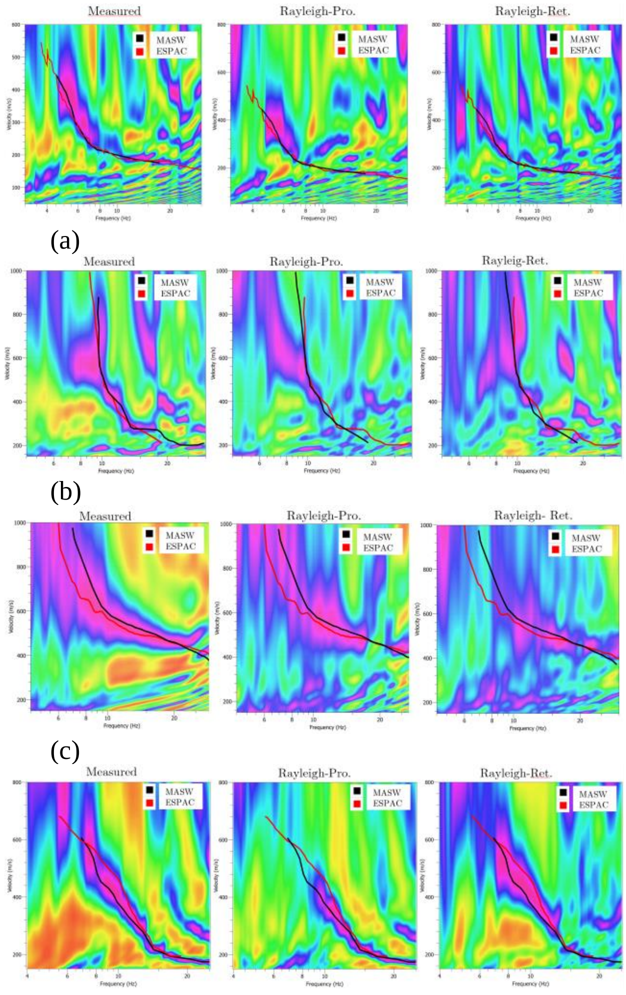

Figure 5. Dispersion curves and f-k spectra for: (a) Site Id 15 – Lighthouse; (b) Site Id 16 – Pedro de Valdivia Park; (c) Site Id 18 – CENDYR; (d) Site 21 – Coquimbo Billboard.

In relation to the total vertical motion measured with the triaxial geophones and the 24 vertical sensors of the Geode® equipment (MASW in Figure 5), the results are quite consistent, especially for frequencies above 6-8 Hz. Below this value, there are some minor differences that may be attributable to the criteria adopted for the identification of the MASW dispersion curve rather than a difference induced by the results of the analysis. In the high frequency range (> 20 Hz), in general, MASW results allow a good description at higher frequencies because the geophone spacing is uniform and more redundant data is available, which improves spatial sampling in the shorter wavelength range. When comparing the results against those from ESPAC, it is observed that, except for site Id 18 (Figure 5c), the results overestimate the dispersion curve below 15 Hz most likely due to the obliquity of the wavefront incidence related to the ambient noise. As previously indicated, site

Id 18 has a non-horizontal stratification, which could explain the trend being different for this site. More detailed analyses are being conducted through computational modelling to better understand the surface wave dispersion properties of these types of stratifications.

On the other hand, a clear reduction of the characterized frequency range is observed when f-k spectrum is obtained from the NIP filtered waveforms. In some cases, the frequency range of the prograde and retrograde Rayleigh waves are very similar (Figures 5a and 5b), while in others they are rather complementary (Figures 5c and 5d), suggesting that the MASW method effectively captures the information available from both polarisations to construct the dispersion curve. Another interesting aspect is that, in general, the dispersion curves from MASW and the f-k spectra from the NIP results are coincident when they provide information in the same frequency range, indicating that the direct use of the total vertical motion does not introduce a significant error when following the usual near-field effect removal procedures. As expected, the f-k spectra from triaxial measurement are less efficient in the higher frequency zone, because the variable spacing between sensors is less effective in characterising shorter wavelengths.

Finally, only for site Id 16 (Figure 5b), the use of the prograde Rayleigh wave indicates a better description of the dispersion properties of the site in the lower frequency region explored (about 6-10 Hz). In this site, the use of this f-k spectrum would have led to lower phase velocities in this range and, therefore, a reduced value of Vs30.

4. Conclusions

This paper presents a study aimed to estimate the uncertainty of active tests based on surface wave methods. For this purpose, conventional MASW active tests were performed in parallel with tests using triaxial sensors that allowed filtering Rayleigh waves from the total recorded motion.

The results showed that, in general, the usual procedures to eliminate the contribution of body waves in the near field are sufficient to avoid an error in the estimation of the dispersion curve produced by non-Rayleigh waves. Except for one of the sites studied, the differences obtained at the dispersion curve level are minor and, therefore, there is no significant error in assuming that all the vertical motion recorded is attributable to Rayleigh waves. However, in the one case where this trend was not verified, the direct use of total vertical motion would lead to a non-conservative characterization of the dynamic properties of the site in terms of Vs30. Complementary analyses are being carried out and more sites need to be characterized to establish indicators, ideally feasible to be evaluated in the field, to anticipate these differences and reduce the probability of obtaining inaccurate dynamic site characterizations.

Results slightly discrepant from the trends were also obtained for a case in which complementary information showed that the site had a non-horizontal stratification. Complementary studies are also required to understand and quantify the differences in the dispersion properties of sites with this type of configuration.

Acknowledgements

This study is based upon work mainly supported by the ANID/FONDEF project ID22I10032. E. Sáez is also supported by CIGIDEN (National Research Center of Integrated Natural Disaster Management) ANID Project 1523A0009 FONDAP 2023.

References

Foti, S., Hollender, F., Garofalo, F. et al. “Guidelines for the good practice of surface wave analysis: a product of the Interpacific project”. *Bull. of Earth. Eng.* 16, 2367–2420, 2018. https://doi.org/10.1007/s10518-017-0206-7.

Greenhalgh, S., Sollberger, D., Schmelzbach, C., and Rutty, M. “Single-station polarization analysis applied to seismic wave1elds: A tutorial. Advances in Geophysics, 59:123–170. 2018. https://doi.org/10.1016/bs.agph.2018.09.002

Hayashi, K. “Development of the surface-wave methods and its application to site investigations”, Ph.D. Dissertation, University of Kyoto, 2008. https://repository.kulib.kyoto-u.ac.jp/dspace/bitstream/2433/57255/1/D_Hayashi_Koichi.pdf

Humire, F., Sáez, E. and Leyto, F. "Manual de aplicación de técnicas geofísicas basadas en Ondas de superficie para la determinación del parámetro parámetro Vs30", *Instituto de la Construcción*, Chile, 2015. https://www.ingeotec.cl/publicaciones/09_19049_manual.pdf

Kværna T. and Ringdahl, F. “Stability of various fk-estimation techniques”, *in Semiannual Technical Summary*. NORSAR Scientific Report 1-86/87, 1986.

Maringue, J., Mendoza, L., Sáez, E. et al. “Geological and geotechnical investigation of the seismic ground response characteristics in some urban and suburban sites in Chile exposed to large seismic threats”. *Bull Earthquake Eng* 20, 4895–4918 (2022). https://doi.org/10.1007/s10518-022-01401-3

Meza-Fajardo, K., Papageorgiou, A. and Semblat, J-F. “Identification and Extraction of Surface Waves from Three-Component Seismograms Based on the Normalized Inner Product”. *Bull of. Seism. Soc. Am.* 105,1, pp. 210-229, 2015. https://doi.org/10.1785/0120140012.

Lacoss, R., Kelly. E. and Toksöz, M. “Estimation of seismic noise structure using arrays”. *Geophysics*, 34, 21-3, 1969. https://doi.org/10.1190/1.1439995

Sollberger, D., Greenhalgh, S. A., Schmelzbach, C., Van Renterghem, C., and Robertsson, J. O. “6-C polarization analysis using point measurements of translational and rotational ground-motion: Theory and applications”. *Geophysical Journal International*, 213(1):77–97, 2018. https://doi.org/10.1093/gji/ggx542

Soto, V. “Numerical simulation of wave propagation in 3D basin models and their effects on nonlinear structures response”. *PhD Dissertation*, Université Paris-Saclay, France, 2023.

Stockwell, R. G., Mansinha, L., and Lowe, R. P. “Localization of the complex spectrum: The S transform”. *IEEE Transactions on Signal Processing*, 44(4):998–1001, 1996. https://doi.org/10.1109/78.492555

Tremblay, S-P. and Karray, M. “Practical considerations for array-based surface-wave testing methods with respect to near-field effects and shear-wave velocity profiles”. *Jour. Appl. Geoph.* 171, 103871, 2019. https://doi.org/10.1016/j.jappgeo.2019.103871.

Wathelet, M. GEOPSY packages (Version 2.5.0), 2002-2011: retrieved from http://www.geopsy.org/download.php

Wathelet, M. "Array Recordings of Ambient Vibrations: Surface-Wave Inversion". *PhD Dissertation*, Liège University, Belgium, 2005.

Yoon, S. and Rix, G.J, "Near-field effects on array-based surface wave methods with active sources". *J. Geotech. Geoenviron. Eng.* 135, 399-406, 2009. https://doi.org/10.1061/(ASCE)1090-0241(2009)135:3(399).